Ice Particle Crystallization in the Presence of Ethanol: An In Situ Study by Raman and X-ray Diffraction

ARTICLE *in* THE JOURNAL OF PHYSICAL CHEMISTRY A · MAY 2013

Impact Factor: 2.69 · DOI: 10.1021/jp4015614 · Source: PubMed

3 AUTHORS:

Sébastien Facq

University of Cambridge

10 PUBLICATIONS **66** CITATIONS

SEE PROFILE

Florence Danède

Université des Sciences et Technologies de Lill…

42 PUBLICATIONS **728** CITATIONS

SEE PROFILE

B. Chazallon

Université des Sciences et Technologies de Lill…

54 PUBLICATIONS **702** CITATIONS

SEE PROFILE

THE JOURNAL OF PHYSICAL CHEMISTRY A

Article

pubs.acs.org/JPCA

Ice Particle Crystallization in the Presence of Ethanol: An In Situ Study by Raman and X-ray Diffraction

Sébastien Facq,[†,§] Florence Danède,[‡] and Bertrand Chazallon[†,*]

[†]Laboratoire de Physique des Lasers, Atomes et Molécules (UMR 8523), Centre d'Études et de Recherches Lasers et Applications (CERLA), Université Lille1, 59655 Villeneuve d'Ascq Cedex, France

[‡]Unité Matériaux et Transformations (UMR CNRS 8207), Université Lille1, 59655 Villeneuve d'Ascq Cedex, France

ABSTRACT: Two distinct ethanol aqueous solution droplets ($(X_{EtOH})_L$ = 8.7 wt % and 46.5 wt %) are investigated by in situ Raman spectroscopy and X-ray diffraction between 253 and 88 K. Structural changes are identified by modifications in the O−H and C−H stretching modes (2800−3800 cm^{-1} spectral region) during freezing and annealing events. They are attributed to the formation of ice and/or different hydrate structures in the EtOH−water system. At high initial ethanol concentration, the particle is found to be composed of a modified clathrate I (cubic structure) at 211 K on cooling and transformed into an ethanol hydrate II (monoclinic structure) on annealing between ∼143 and 173 K. This latter decomposes at ∼200 K and leaves an aqueous solution and ice Ih which further dissociates above ∼230 K. At low initial concentration, ice first forms on cooling and the particle consists of a crystalline ice core embedded in a liquid layer of high ethanol content at ∼200 K (or an amorphous layer at lower T). A new hydrate (IV) of distinct structure (orthorhombic) is observed on annealing (from 100 K) between ∼123 K and ∼142 K (depending on initial composition), which transforms into the ethanol hydrate II at ∼160 K. The hydrate II decomposes at ∼200 K, and ice Ih remains (and dissociate above ∼220 K) in coexistence with the liquid layer of high ethanol content. It is proposed that the complex crystalline ice particles formed may have the potential to impact several atmospherical processes differently in comparison to the pure ice case.

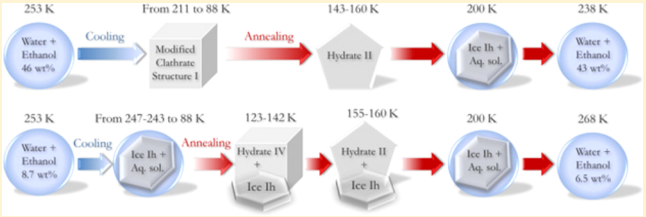

1. INTRODUCTION

1.1. Outline. The behavior of aqueous solutions at low temperature has been and is still widely examined because of its importance in many fields of research such as cryopreservation of living cells and organs,[1] cryoprotection, and antifreeze protection of biological species[2] or atmospheric physico-chemical processes.[3−10] In the atmosphere, aqueous solutions may exist at temperatures lower than 230 K in mixed clouds which both contain ice crystals and supercooled droplets or in deep convective clouds.

The behavior of supercooled droplets of aqueous solutions of dissolved volatile organic compounds during cooling and the determination of the crystalline structures formed are essential for a better understanding of the creation of the new ice particles. Indeed, many biological or atmospheric properties and processes may be affected by crystallization effects. This will depend on the particle sizes, on their chemical compositions, and also on the surface state which drives ice reactivity especially in the atmosphere.

In the past, many studies have focused on the freezing process of the EtOH−water system using X-ray diffraction, thermal analysis, or dielectric measurements.[11−18] They have highlighted the presence of many ethanol hydrates in the phase diagram of the EtOH−water system, however, without giving a clear picture of the number, the composition, and the structure of theses hydrates. Besides, recent advances provided by an alternative trapping process allow investigating a specific part of the phase diagram relevant to the atmospheric purposes.[19−21]

1.2. Physical Background of the Freezing Behavior of Particles According to the Ethanol−Water Phase Diagram. The behavior of the freezing of ethanol aqueous solutions of 8.7 and 46.5 wt % may be predicted from the EtOH−water phase diagram. However, the construction of such a diagram is quite complex given the discrepancies in the number, composition, and dissociation temperature of the different ethanol hydrates from literature.[11−18] Detailed information on the melting temperature, stoichiometry, and structure about these hydrates is summarized in Table 1. It can be seen that a modified structure II clathrate (CS−II) is observed in a broad range from 20 to 32 wt % in earlier studies,[13] whereas other authors report the occurrence of structure I clathrate (CS−I) in the range 0−35 wt %.[16] Further, the number of hydration differs among the different authors between 1.2 and 17 without a clear separation in the domain of existence.

In Figure 1, we show the phase diagram (thermodynamic) of the ethanol−water system as determined by Takaizumi and Wakabayashi[14] (linked open circles). The glass transition temperature (T_g) as a function of ethanol concentration is

Received: February 13, 2013
Revised: May 16, 2013
Published: May 17, 2013

   dx.doi.org/10.1021/jp4015614 | J. Phys. Chem. A 2013, 117, 4916−4927

Table 1. Stoichiometry, Dissociation Temperature, Existence Domain, and Structure of Ethanol Hydrates Reported in Literature[a]

composition	melting T [K]	domain of existence [wt %]	structure	refs
E·5H_2O	199	0−80	N.C.	11
E·17H_2O	199.5	11.55−64.8	modified cubic CS−II	12
E·17H_2O	198.5−204	20−32	modified cubic CS−II	13
E·(7.67−5.75H_2O)	206−212.5	35−70	cubic CS−I	13
E·(5.67−17)H_2O	199.1−201.5	0−31.1	cubic CS−II or CS−I	14
E·4H_2O	226	31.1−39	N.C.	14
E·2H_2O	221	39−56.1	N.C.	14
E·1.2H_2O	208	68.1−94	N.C.	14
N.C.	210.4	N.C.	cubic CS−I (?)	15
N.C.	199.5	N.C.	cubic CS−II	15
E·4.75H_2O	198.5	0−35	cubic CS−I	16
E·3H_2O	204	35−46	N.C.	16
E·2H_2O	208	46−56.1	N.C.	16
E·4H_2O?	N.C.	39−52.3	N.C.	17
E·(4.67−4.75)H_2O	208.5−210	31−66	cubic CS−I or CS−II	18
E·2.2H_2O	198−210	9−65.4	N.C.	20
E·(7.67−4.75H_2O)	158−193	9−65.4	modified cubic CS−I	20
E·(4.75−5)H_2O	198	23.8−37.2	N.C.	21
E·2H_2O	208	37.2−65.4	tetragonal	21

[a]CS−I and CS−II stand for cubic structures I and II, respectively, and N.C. for not communicated by the authors. The "?" corresponds to an uncertainty on the determination of the structure.

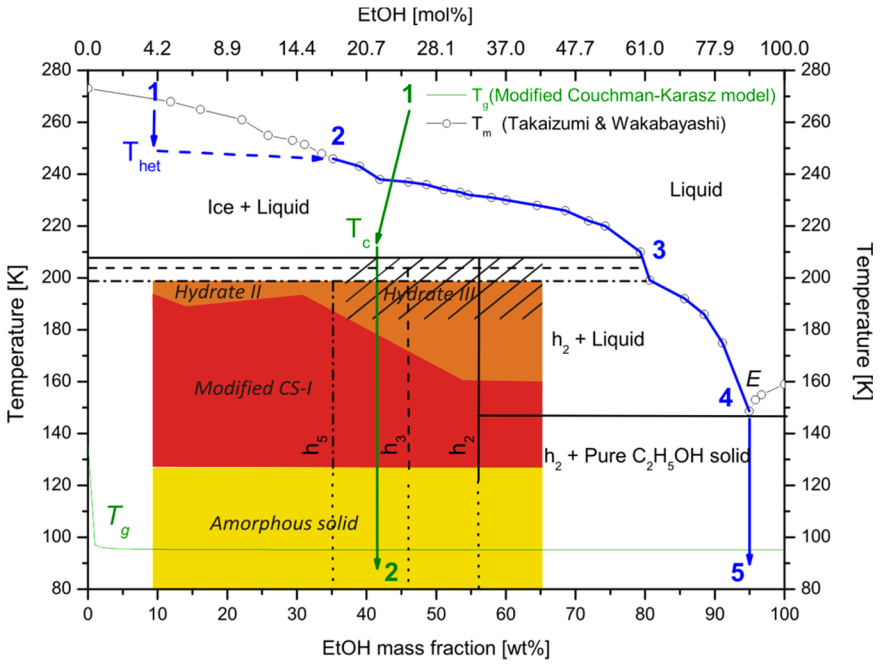

Figure 1. Phase diagram of the EtOH−water system. Melting temperatures of the ethanol−water system are taken from Takaizumi and Wakabayashi[14] (linked open circles). The green solid line represents the glass transition temperature estimated from the modified Couchman−Karasz model.[22] The four horizontal lines located at 208, 204, 198.5, and 148.5 K represent the four temperature invariants determined by Zelenin.[16] The first three invariants correspond to the melting of peritectic hydrates of composition E·(2 ± 0.2 H_2O) (h_2 = hydrate III), E·(3.2 ± 0.3 H_2O) (h_3 = not observed by us), and E·(4.9 ± 0.4 H_2O) (h_5 = hydrate II). The fourth temperature invariant corresponds to the melting of the eutectic hydrate E·(2 ± 0.2 H_2O) and pure solid ethanol. The location of hydrate IV is not given as the stoichiometry has not been determined. Phases in italic are formed from annealed vapor deposited solid films or by direct co-deposition at 183 K obtained from our previous work.[19−21] Their domains of existence are indicated by the colored and hatched areas. Thermal treatment trajectories are displayed through numbers 1 to 5 in blue (dotted lines, 8.7 wt % sample) and through numbers 1 to 2 in green (dotted lines, 46.5 wt % sample).

shown as a green solid line. This is estimated from the modified Couchman−Karasz model.[22] Four temperature invariants determined by Zelenin[16] and located at 208, 204, 198.5, and 148.5 K are also presented as horizontal lines. The first three invariants correspond to the melting of peritectic hydrates of composition E·(2 ± 0.2 H_2O) (h_2), E·(3.2 ± 0.3 H_2O) (h_3), and E·(4.9 ± 0.4 H_2O) (h_5), according to Zelenin's nomenclature. The fourth temperature invariant corresponds to the melting of the eutectic hydrate E·(2 ± 0.2 H_2O) and pure ethanol solid. Vertical lines correspond to the concen-

dx.doi.org/10.1021/jp4015614 | J. Phys. Chem. A 2013, 117, 4916−4927

tration's domain of existence of these hydrates. The domains of existence of ethanol hydrates formed from annealed vapor deposited solid films (colored areas) or by direct co-deposition at 183 K (colored and hatched areas) are obtained from our previous work.[19−21]

According to Takaizumi and Wakabayashi,[14] the first solid formed during cooling of an EtOH aqueous solution of concentration lower than 34.4 wt % is ice. Upon further cooling, the behavior is quite more complex. Taking an ethanol aqueous solution of 8.7 wt %, this one should freeze heterogeneously at T_{het} (Figure 1). At this temperature, a phase separation should occur between water and ethanol: hexagonal ice is formed and ethanol present in excess is removed from the growing ice phase to form an aqueous solution of higher concentration (landmark 2 in blue). This behavior has already been mentioned during freezing under atmospherically relevant cooling rate of many organic/inorganic aqueous solutions of high molecular weights.[23] Upon further cooling, the ethanol content of the supercooled aqueous solution increases as temperature decreases to reach the first temperature invariant at 208 K on the melting curve (landmark 3 in blue). At this point, a part of the solution should crystallize into an ethanol hydrate. The remaining aqueous phase continues to concentrate until the fourth temperature invariant located at 149 K (landmark 4 in blue) is reached. At this point, a pure ethanol solid (landmark 5 in blue) should form. So the ice particle expected during the freezing of an ethanol aqueous solution of 8.7 wt % should have a complex structure constituted mainly of hexagonal ice and two distinct ethanol hydrate structures.

For an ethanol aqueous solution of concentration higher than 34.4 wt %, the first solid formed during cooling is an EtOH hydrate[14] which crystallizes at T_c. All or most of the ethanol present in solution is then trapped in the newly formed solid particle. If the ethanol hydrate is stable, the composition of this solid particle should not vary too much upon further cooling (landmark 2 in green). A remaining solution may exist with a composition close to the eutectic. However, according to Zelenin's phase diagram, it is suggested that the first hydrate should co-exist with a second hydrate to form a solid particle without any liquid phase.

The aim of this study is to examine the behavior of supercooled droplets of EtOH aqueous solutions and determine the structures formed during cooling on a wide temperature range (253−88 K) in order to cover a large part of the EtOH−water phase diagram. As thermodynamic equilibrium is not always reached on a first cooling, the behavior of the ice particles has also been investigated during annealing (a situation that may be comparable to the temperature fluctuations in the atmosphere). Because the first solid formed during cooling of an EtOH aqueous solution of concentration lower than 34.4 wt % is supposed to be ice whereas it is an EtOH hydrate above this value,[14] we examine these two important distinct cases. We perform micro-Raman analysis and X-ray diffraction during cooling and annealing of two EtOH aqueous solution droplets of 8.7 and 46.5 wt %. These two distinct cases are studied in detail below.

2. EXPERIMENTAL METHODS

2.1. Sample Preparation. Ethanol aqueous solutions of composition $(X_{EtOH})_L$ = 8.7 and 46.5 wt % are prepared with pure ethanol purchased from Verbièse (France) (purity > 9.77%) mixed with double-distilled and deionized water (resistivity ≈ 8 MΩ·cm^{-1}) produced by a water purifier (UHQ PS (Elgastat)) and then stored in our cold room maintained at 264 K. Using a micropipet, 0.5 μL of aqueous solution (providing a droplet radius of 600−800 μm depending on the ethanol content) is introduced into a "homemade" sample cell and placed inside a dedicated cryostage (Linkam). The sample cell consists of two borosilicate coverslips (22 mm in diameter, 130−170 μm base thickness) and a Viton silicon ring about 1.7 mm thick with an inner diameter of about 2 mm. The sealing between the coverslips and the silicon ring is obtained by two layers of high vacuum grease (Dow Corning). After droplet deposition, both the sample cell and the cryostage are quickly sealed. This operation is entirely done in the cold room in order to limit ethanol evaporation during the preparation.

The cryostage is then cooled down to 88 K at cooling rate of 0.7 K·min^{-1} using a controlled liquid nitrogen flow (precision of ±0.1 K) and then annealed at heating rate of 0.7 K·min^{-1} up to 268 K. This cooling rate has been chosen to be representative of a typical cooling rate observed during cirrus formation.[24] Each run was repeated to test the reproducibility of the phase change phenomena in different solutions. Before each one, the concentration of the ethanol aqueous solution is controlled by micro-Raman spectroscopy using a calibration curve. This latter has been obtained from spectra collected on reference solutions maintained at equilibrium in a sealed capillary tube at ambient temperature. It relates the ethanol concentration ($(X_{EtOH})_L$= 2.5−63 wt %) to the relative ratio of ethanol C−H and water O−H integrated Raman bands. The experimental results are displayed in Figure 2, as well as a linear correlation with our data (R = 0.99969).

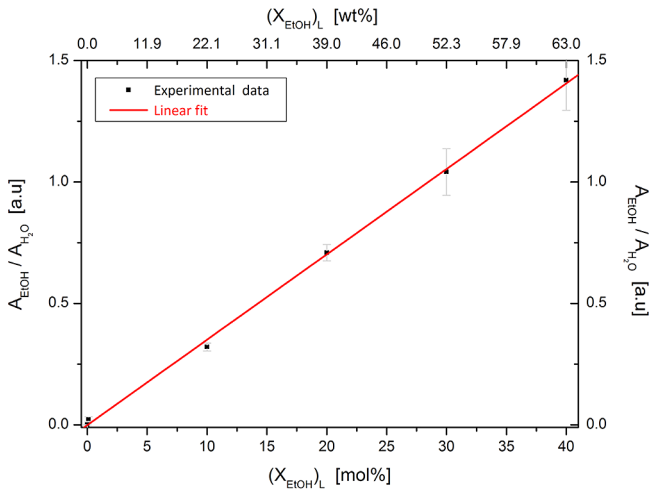

Figure 2. Ratio of the integrated area of EtOH C−H and water O−H bands in aqueous solutions of concentration 2.5 wt % < $(X_{EtOH})_L$ < 63 wt % (filled squares) and the corresponding linear fit (red curve).

2.2. Micro-Raman Measurements. We use an Invia Reflex Raman spectroscope (Renishaw) with a 250 mm focal length equipped with an Olympus BXFM free-space microscope on which the cryo-stage is mounted. A spectral resolution of ∼1.5 cm^{-1} is reached with a holographic grating of 1800 grooves·mm^{-1} and a Peltier cooled front illuminated CCD detector (576 × 400 pixels). The excitation radiation (λ = 514.5 nm) is produced by an Ar^+ laser source (Modulaser). An Olympus 50× objective LWD (0.5 N.A.) provides a ∼1 μm circular beam spot. The laser power at sample is 4 mW as

dx.doi.org/10.1021/jp4015614 | J. Phys. Chem. A 2013, 117, 4916−4927

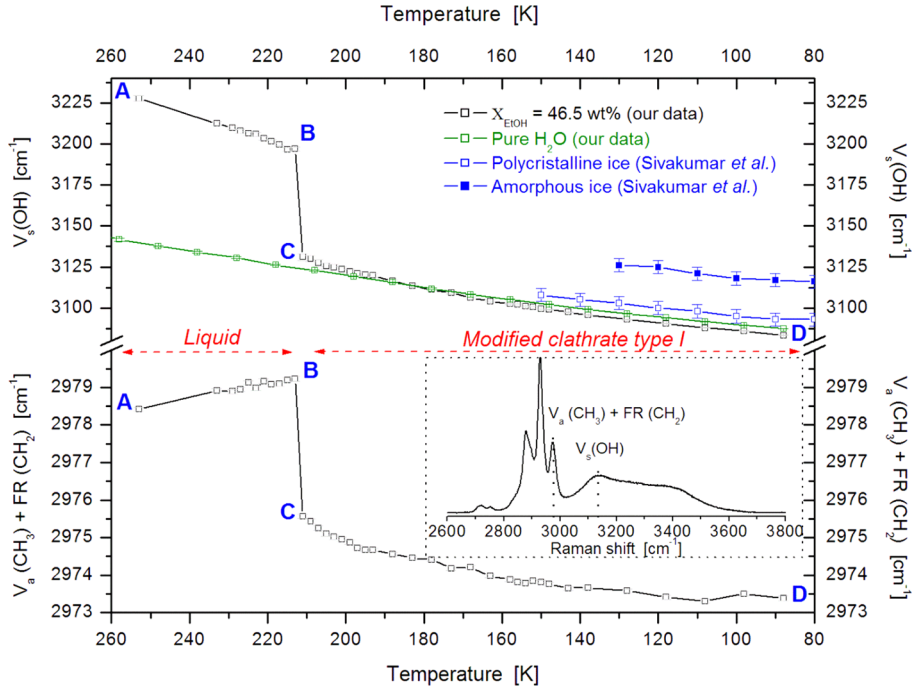

Figure 3. Top: Frequency evolution during cooling from 253 to 88 K of the ν_S(OH) band for hexagonal and amorphous ice (open blue squares and filled blue squares, respectively), pure crystalline ice formed from liquid (open green squares) as well as for a 46.5 wt % EtOH aqueous solution (open black squares). Bottom: Frequency evolution during cooling from 253 to 88 K of the $\nu_A(CH_3)$ and FR(CH_2) band for a 46.5 wt % EtOH aqueous solution (open black squares).

measured by a Lasercheck powermeter (Coherent). Spectral positions were calibrated against the silicon line, yielding a stable value of 520.4 ± 0.3 cm^{-1}. Raman spectra are collected during the cooling and annealing protocol in the spectral region of ethanol C−H and water O−H vibrational stretching modes. They are baseline-corrected, and the peak positions are determined using a least-squares fitting procedure.

2.3. X-ray Measurements. The powder X-ray diffraction (PXRD) experiments were performed with an Inel CPS 120 diffractometer ($\lambda_{CuK\alpha}$ = 1.54056 Å) equipped with a 120° curved position sensitive detector coupled to a 4096 channel analyzer. The samples are inserted into Lindemann glass capillaries (Ø = 0.7 mm) and processed at a cooling rate of 1 K·min^{-1} starting from the liquid. The same heating rate is applied. Bragg reflections are indexed and refined using the EXPO 2004 software.[25]

3. RESULTS AND DISCUSSION

3.1. Freezing of a 46.5 wt % Ethanol Aqueous Solution. *3.1.1. O−H Stretching Mode.* The ethanol and water O−H vibrational stretching modes are particularly sensitive to intra- and intermolecular interactions in ice crystal. Frequency changes in the position of these modes may provide information about intermolecular coupling and anharmonicity as well as H bond local geometry.[26] A detailed assignment of the bands corresponding to the O−H bond stretching modes in hexagonal and cubic ice has been proposed by E. Whalley[27] using comparison of Raman spectra of these two phases with those of ice VII and VIII. In this study, the most intense band of the spectrum, located around 3083 cm^{-1}, is attributed to the symmetric stretching mode ν_1 "in phase" (i.e., where the water molecules execute a ν_1 vibration in phase with each other). This band is followed by a weaker one at 3209 cm^{-1} attributed to the anti-symmetric stretching mode ν_3 transverse-optic and two other large bands located at 3323 cm^{-1} and 3420 cm^{-1}, respectively. Of these last two, the former one is assigned to the anti-symmetric ν_3 longitudinal-optic and the latter one is suggested to be the symmetric stretching mode ν_1 "out of phase" (i.e., where the water molecules execute a ν_1 vibration out of phase with each other).

Temperature dependence of these modes as well as their full width at half-maximum has been studied by Sivakumar et al.[28] for hexagonal and amorphous ice formed by deposition from the vapor phase at 150 and 10 K, respectively. The temperature dependence of the O−H symmetric stretching mode ν_1 "in phase" (referred here as ν_S(OH)) for hexagonal and amorphous ice (open blue squares and filled blue squares respectively) and pure crystalline ice formed from liquid (open green squares, our data) as well as for the 46.5 wt % aqueous solution (open black squares, our data) is shown in Figure 3 (top).

The ν_S(OH) band position of pure crystalline ice (our data and from Sivakumar et al.[28]) and amorphous ice[28] are plotted as reference data in order to compare with the behavior of our aqueous solution during cooling. The ν_S(OH) band position of pure crystalline ice formed from liquid (open green squares, our data) is in relatively good agreement with the Sivakumar et al.[28] results (open blue squares), with a small difference observed (for instance, ∼3093.6 cm^{-1} for Sivakumar et al.[28] against ∼3088.6 cm^{-1} for us at 90 K) which is attributed to the large experimental uncertainties that these authors report for their absolute frequencies (±4 cm^{-1}). Nevertheless, these two curves follow the same trend, i.e., an evolution with temperature of $\partial\omega/\partial T \sim -0.23$ cm^{-1}·K^{-1} (between 150 and 80 K), which is in excellent agreement with previous works.[28,29] This thermal effect is generally attributed to a volume decrease with temperature and partially reflects the strengthening of H bonds between ethanol and water molecules when temperature

dx.doi.org/10.1021/jp4015614 | J. Phys. Chem. A 2013, 117, 4916−4927

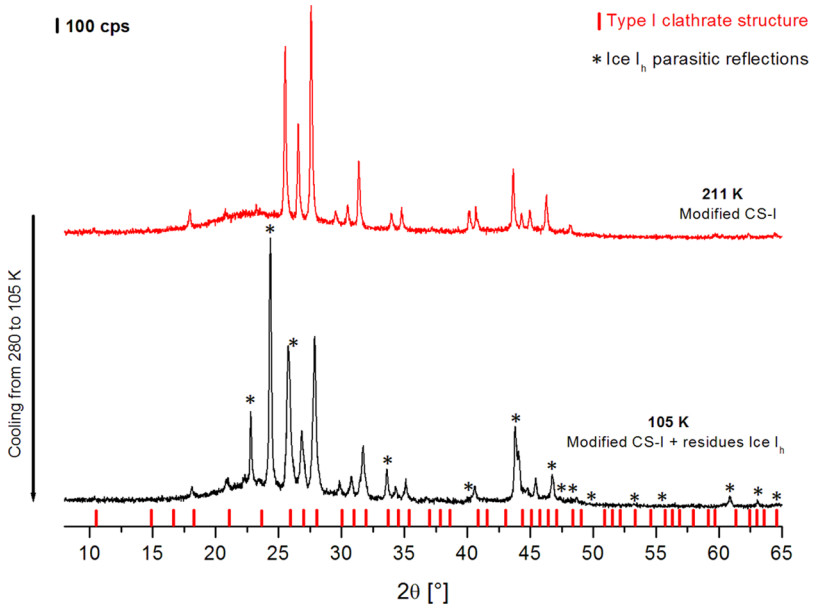

Figure 4. Diffraction pattern of a 46.5 wt % sample (initial composition) recorded at 211 K (red line) and 105 K (black line) during cooling (and indexed as a modified type I, S.G. *Pm*3*m*). Asterisks represent parasitic reflections of Ice Ih present at the surface of the Lindemann capillary at 105 K. Red tickmarks represent expected reflections for a clathrate type I (derived from Yousuf et al.[32] at 90 K).

decreases. Other coupling effects such as a strong intermolecular coupling, anharmonicity of linked water molecules, or H bond specific local geometries must also be taken into account.[26] A significant blue-shift of ∼30 cm^{-1} (in the range 80 K < *T* < 130 K) is shown when the crystalline ice data are compared to that of amorphous ice (filled blue squares). This shift reflects a strengthening of the O−H bond in the crystalline structure when compared to amorphous ice. The same behavior is observed in our EtOH aqueous solution and suggests that the frozen solution has a crystalline structure in this temperature range.

Between 253 K (point A) and 213 K (point B), the significant decrease (slope of $\partial\omega/\partial T \sim -0.8$ $cm^{-1}\cdot K^{-1}$) reflects a ν_S(OH) band shift from ∼3197 cm^{-1} to ∼3228 cm^{-1} attributed to a H bond strengthening between ethanol and water molecules in the liquid during cooling. Then, a steep red-shift of ∼66 cm^{-1} between 213 and 211 K (between points B and C) indicates the crystallization of the sample. This well-known effect reflects a difference of local structure and bond in the liquid with the presence of weaker H bonds when compared to the solid state. Moreover, a small but significant difference between the ν_S(OH) band position in pure crystalline ice (open green squares) and in the frozen aqueous solution (open black squares) is observed below 211 K. The frozen solution plot intercepts the crystalline ice plot at ∼178 K with a frequency difference that increases up to ∼4 cm^{-1} as temperature decreases down to 88 K. This additional shift is attributed to the formation of an ethanol hydrate in which the H bonds between ethanol and water molecules may be of different nature compared to those in pure ice. The X-ray diffraction work presented below corroborates the existence of a distinct structure relative to ice, with the formation of a clathrate (or possibly a semi-clathrate) which causes modifications in H-bond strengths and in ν_S(OH) band position. A similar behavior has been reported in annealed vapor-deposited water−ethanol thin films.[19]

3.1.2. C−H Stretching Mode. A confirmation of the above statement is observed in the ethanol C−H stretching modes which are also good indicators of structural changes and sensitive to modification in H bond strengths and changes in ethanol concentration in the liquid phase.[19,21] As described elsewhere,[30] all C−H stretching modes shift to lower frequencies as $(X_{EtOH})_L$ increases due to a partial and gradual electron transfer from the hydrogens and carbon to the oxygen of the EtOH molecule to participate in H bond formation. A drop in frequency will therefore indicate H bonds formation due to an increase of the ethanol content in the solution or the formation of a crystalline compound when a solid is formed. The C−H stretching modes are composed of three main bands located at ∼2876 cm^{-1}, ∼2928 cm^{-1}, and ∼2973 cm^{-1} for pure liquid ethanol. A detailed assignment of these components has been given by Yu et al.[31] and is taken as reference here. Only the evolution of the band at ∼2973 cm^{-1} assigned to both the symmetric $-CH_2$ Fermi resonance mode and the weak $-CH_3$ antisymmetric stretching mode [$\nu_A(CH_3)$ and $FR(CH_2)$][31] is displayed as a function of temperature in Figure 3 (bottom).

A small increase of frequency between point A and B is attributed to a partial evaporation of ethanol on cooling. Frequency shifts of respectively ∼3.7 cm^{-1}, ∼1.2 cm^{-1}, and ∼3.1 cm^{-1} are observed for the three C−H bands between 213 and 211 K (between point B and C). This confirms the formation of a crystalline solid in which the C−H bond lengths are disturbed by changes in molecular local environment around ethanol molecules. The occasional H bond formation between ethanol molecules and water molecules forming the clathrate cage (see below) may be responsible for these shifts. No other noticeable modification is observed upon further cooling, except a progressive frequency drop between 211 and 88 K (point C and D) due to H bond strengthening with temperature. The ethanol hydrate is apparently stable during cooling down to 88 K.

3.1.3. X-ray Diffraction Measurements. The X-ray measurements allow the identification of the structure suggested by the Raman experiments. The formation of an ethanol hydrate is observed at ∼211 K (Figure 4). Most of the reflections can be indexed in terms of a cubic structure. A refinement of the

dx.doi.org/10.1021/jp4015614 | J. Phys. Chem. A 2013, 117, 4916−4927

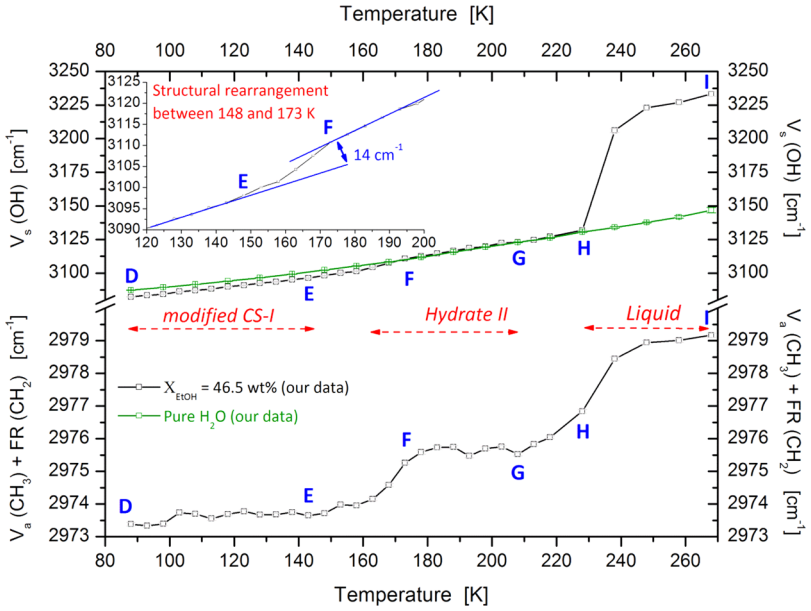

Figure 5. Top: Frequency evolution during annealing from 88 to 268 K of the ν_S(OH) band for pure crystalline ice formed from liquid (open green squares) and a 46.5 wt % EtOH aqueous solution (open black squares). Bottom: Frequency evolution during annealing from 88 to 268 K of the $\nu_A(CH_3)$ and FR(CH_2) band for a 46.5 wt % EtOH aqueous solution (open black squares).

pattern gives the space group of *Pm*3*m*, which is closely related to that of the type I clathrate (CS−I) of *Pm*$\bar{3}$*n* space group. The refined lattice parameters give a unit cell dimension of a = 12.091 Å at 211 K relatively close to the experimental values reported by Boutron and Kaufmann.[13] However, these authors interpreted their diffraction patterns in terms of the space group of *Pm*$\bar{3}$*n* (CS−I with a = 11.9 Å at 77 K) whereas their samples were obtained from quenched solutions of similar composition of ∼45 wt %. In contrast, a modified ethanol type I clathrate has been reported more recently at ∼138 K during annealing of ethanol−water mixtures co-deposited from the vapor phase at low temperature.[20] Note that in comparison to the expected lines of a type I clathrate of methane (red tickmarks),[32] about eight lines are missing or are very weak. We therefore assume here that our experimental X-ray pattern corresponds to a modified type I and not a "true" type I as previously assumed by Boutron and Kaufmann. The ethanol concentration of the frozen aqueous solution estimated from our Raman measurements after crystallization (211 K) is about 41.3 wt % which corresponds to a hydration number of 3.63 (±0.6 H_2O). This value is lower than that expected for type I clathrate (between 7.67 to 4.75 H_2O). The value of 7.67 corresponds to a clathrate where the guest occupies only the large cages, 5.75 is for a full occupation of both the large and small cages, and 4.75 is obtained by replacing one water molecule by one guest molecule in all the cages.[18] The hydration number of 3.63 found by Raman corresponds to an excess of ethanol which is probably removed from the crystalline (modified) clathrate phase and remains under a non-crystalline state (and may contribute to the broad shape of the background in the pattern Figure 4). In their work, Boutron and Kaufman[13] mentioned that a part of their solution will have the composition of the eutectic and remains amorphous even at low temperature when their "clathrate I" crystallizes. The hydration number value derived from our Raman spectra thus represents an average composition of both contributions (crystalline and non-crystalline) and is probably underestimated in the modified clathrate I. Since the small cage size is on the limit of accepting the ethanol molecule (of propane-sized), the composition may be close to E·7.67H_2O with occasional bonding to the cage wall. In contrast, Zelenin assigns the CS−I of Boutron and Kaufmann to the stable phase of hydrate h_S they reported (with E·4.9H_2O) and supposes that the ethanol intercalates into the water framework with a full occupancy of the cavities. Our results do not support this conclusion as the modified type I is a metastable phase which vanishes on annealing (see below). Upon further cooling, no modification of the sample structure is observed down to 105 K. As no other hydrates crystallize, the hypothesis derived from Zelenin's phase diagram (see Introduction) seems not consistent within the kinetics and temperature trajectories applied here.

3.2. Annealing of the 46.5 wt % Ethanol Aqueous Solution. *3.2.1. O−H and C−H Stretching Modes.* Structural changes observed during annealing are revealed by the spectral modification in the water O−H and ethanol C−H stretching modes (Figure 5). First, a progressive increase $\partial\omega/\partial T \sim 0.26$ $cm^{-1}\cdot K^{-1}$ in the ν_S(OH) band position is observed between 88 and 143 K (point D and E). It is attributed to H bonds softening with temperature. The modified type I clathrate formed on cooling remains present during annealing up to 143 K. Second, from 143 K (point E) to 173 K (point F), a change of slope of $\partial\omega/\partial T \sim 0.48$ $cm^{-1}\cdot K^{-1}$ appears, and the ν_S(OH) band position shifts to more than 14 cm^{-1} in this temperature range and intercepts the evolution of the OH curve of pure ice (see Figure 5). Correspondingly, a blueshift of ∼1.9 cm^{-1}, ∼1.1 cm^{-1}, and ∼0.5 cm^{-1} is observed in the C−H stretching band positions. Such changes are representative of a structural rearrangement in the crystalline phase during annealing. The added mobility gained by the thermal treatment applied promotes H bonds breaking and a rearrangement inside the crystalline phase in order to form new H bonds of the same strength as those in pure ice. Above 173 K (point F) and until ∼200 K, a progressive increase of $\partial\omega/\partial T \sim 0.37$ $cm^{-1}\cdot K^{-1}$ is observed in the ν_S(OH) band position. It is attributed to H bonds softening between ethanol and water molecules. In this interval, a frequency "plateau" is observed in the C−H band

dx.doi.org/10.1021/jp4015614 | J. Phys. Chem. A 2013, 117, 4916−4927

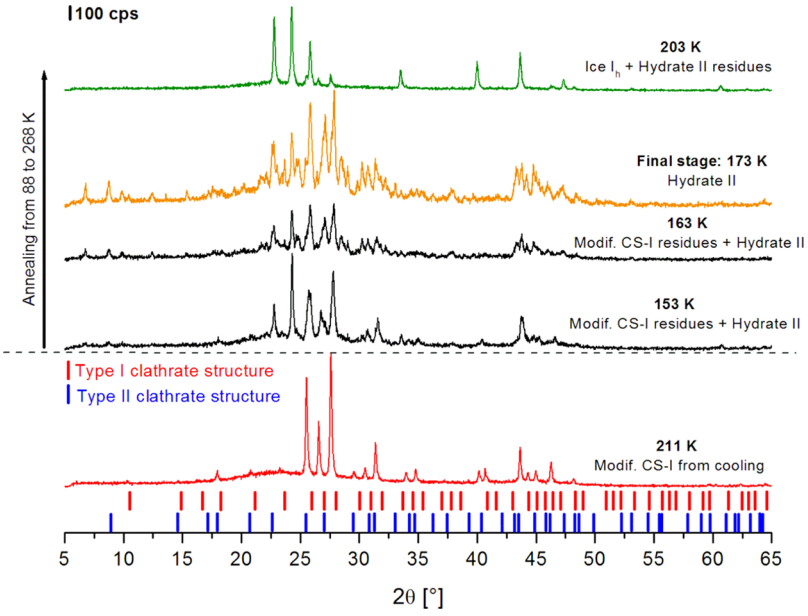

Figure 6. Diffraction pattern of a 46.5 wt % sample (initial composition) recorded at 211 K during cooling (red line) and during annealing at 153 K, 163 K (black lines), 173 K (orange line, hydrate II), and 203 K (green line, ice Ih). Red and blue tickmarks represent expected reflections for a clathrate type I and type II, respectively (derived from Yousuf et al.[32] at 90 K).

(point F to G, Figure 5) and suggests the formation of a distinct hydrate. A frequency drop is then shown between ∼200 and 228 K (point G and H, Figure 5), which reflects the dissociation of the hydrate. At this step the sample is composed of ice and an aqueous solution of ethanol (see also below Section 3.2.2). Between 228 and 238 K (point H and I), a steep redshift (∼74 cm^{-1}) is observed in the ν_S(OH) band position which is assigned to the melting of hexagonal ice. Between 238 and 268 K, a partial evaporation of ethanol from the liquid solution may explain the evolution of the ν_S(OH) band position as well as H bonds softening. The same reasoning is adopted to explain the behavior of the C−H band.

3.2.2. X-ray Diffraction Measurements. In Figure 6, the results obtained from X-ray measurements are displayed for comparison. The diffraction patterns are collected during annealing of the 46.5 wt % ethanol−water mixture. The modified clathrate type I present at 100 K remains stable until 143 K. Then at 153 K, additional peaks progressively start to grow while the modified type I clathrate peaks decrease. This evolution establishes its final stage at 173 K (Figure 6). When comparing with the Raman results (points E and F in Figure 5), these modifications occurred in the same temperature range thus proving the consistency of our methods. In their X-ray diffraction measurements of quenched cooled aqueous solutions of similar composition (∼45 wt %), Boutron and Kaufmann[13] have observed the occurrence of many new distinct lines during warming above 179−200 K (depending on the warming rate) in the diffraction pattern of their "clathrate I" beside the pre-existed ones. They explained the presence of these lines by the ordering of the ethanol molecules that form a lattice in the clathrate cages which is periodic above much longer distances than that of the cages. Our interpretation is here different, as only few lines but not all the lines of the modified clathrate I overlap with those of the newly formed structure at 173 K. We then compared the hexagonal ice Ih, the tickmarks of clathrate type I and II derived from the space group $Pm\bar{3}n$ and $Fd\bar{3}m$[32] and the modified clathrate type I in Figure 6. It appears that all the reflections of our 173 K diffraction pattern can be indexed in terms of the ethanol hydrate II which was recently reported on co-deposited ethanol−ice films at 183 K.[21] This hydrate II has also been obtained from amorphous films deposited at 88 K and annealed between 158 K and 188−193 K (depending on the ethanol content).[19,20] In the former case, the ethanol hydrate II is obtained by direct co-deposition at 183 K of gas mixtures of concentration between $(X_{EtOH})_S$ = 23.8 and 37.2 wt %.[21] The hydrate II was shown to be a stable phase in contrast to the modified clathrate type I.[21] The calculation of the peak indexing procedure performed on the frozen solution suggests that the crystal structure is probably monoclinic with a space group *P*2/*m*. The lattice constants derived from these data (figure of merit M'20 = 36) are a = 20.78 Å, b = 7.01 Å, and c = 12.78 Å and $\alpha = \gamma = 90°$ and $\beta = 101.3°$. Thus, this hydrate has to be distinguished from all previously known ethanol hydrate structures reported in the literature.[13−18] In particular, about 25 additional Bragg lines are observed in comparison to the Bragg reflexions of the "modified CS−II" reported by Boutron and Kaufmann. On this basis and given the range of existence of this hydrate, we attribute Zelenin's stable h_5 (E·4.9 H_2O) to our hydrate II, in accordance with our previous assumption.[21] By further annealing to 203 K, the diffraction pattern mainly shows peaks representative of hexagonal ice with a small residual contribution of ethanol hydrate II peaks that are being dissociated.

In summary, a type I clathrate (possibly modified) of composition close to 7.67 H_2O is formed at ∼211 K on cooling of an ethanol aqueous solution of initial concentration of 46.5 wt %. The structure refinement of the diffraction pattern gives a cubic unit cell with a $Pm3m$ space group. This hydrate forms during cooling down to 88 K and remains present upon annealing up to 143 K. A structural rearrangement is then observed between 143 and 173 K corresponding to the formation of the ethanol hydrate II of crystal structure possibly close to monoclinic and reported previously.[20,21] This latter dissociates below ∼203 K and only ice Ih + an aqueous solution remain. Note that a small ice quantity may also have formed

dx.doi.org/10.1021/jp4015614 | J. Phys. Chem. A 2013, 117, 4916−4927

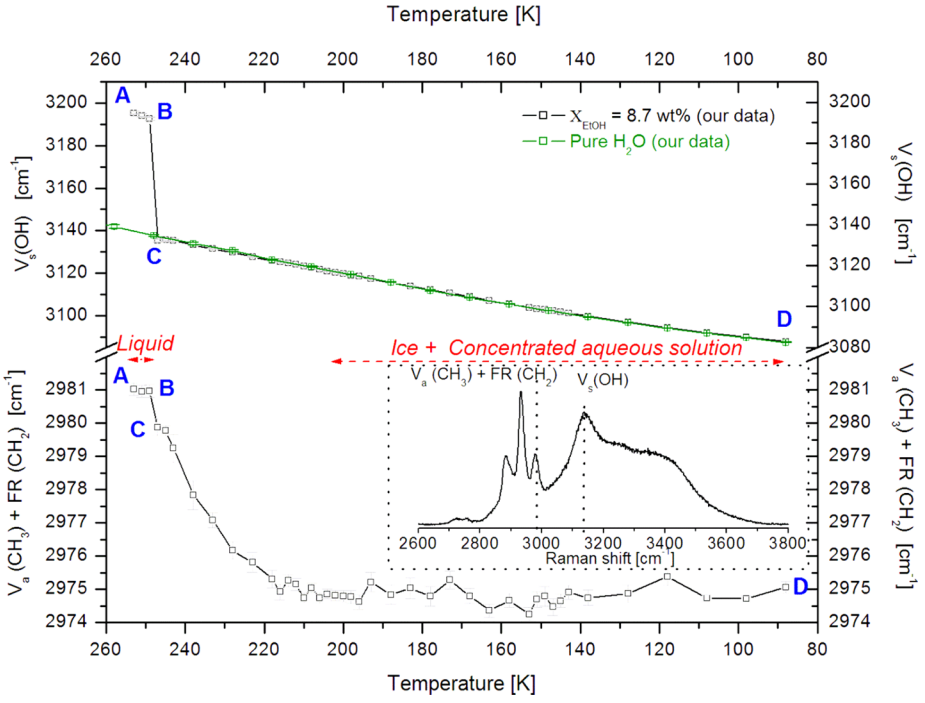

Figure 7. Top: Frequency evolution during cooling from 253 to 88 K of the ν_S(OH) band for pure crystalline ice formed from liquid (open green squares) and a 8.7 wt % EtOH aqueous solution (open black squares). Bottom: Frequency evolution during cooling from 253 to 88 K of the $\nu_A(CH_3)$ and FR(CH_2) band for a 8.7 wt % EtOH aqueous solution (open black squares).

during the transformation of the modified CS−I into the hydrate II. We suggest that the structures given by Boutron and Kaufmann for the solid they formed using a ∼45 wt % mixture by quenching may have been erroneously attributed to a true type I (CS−I). Further, the structural ordering of ethanol in the cavities during annealing is not supported by us.

3.3. Freezing of the 8.7 wt % Ethanol Aqueous Solution. *3.3.1. O−H and C−H Stretching Modes.* A frequency drop of $\partial\omega/\partial T \sim -0.7$ $cm^{-1}\cdot K^{-1}$ is first observed in ν_S(OH) between 253 and 249 K (points A and B, Figure 7). It is attributed to a volume decrease with temperature and partially reflects an H-bond strengthening as temperature decreases. The formation of ice is then observed through spectral changes in the water O−H and C−H stretching modes. A steep frequency shift of ∼57 cm^{-1} takes place between 249 and 247 K (points B and C, Figure 7) which indicates the crystallization of hexagonal ice. In contrast to the sample at 46.5 wt % (Figure 3), there is a perfect match of the ν_S(OH) band position with that of the one of pure hexagonal ice (open green squares) from 247 K (point C) to 88 K (point D), thus corroborating mainly ice formation.

A similar ascription can be derived from the evolution of $\nu_A(CH_3)$ and FR(CH_2) band frequency which decreases between 249 and 247 K (points B and C, Figure 7). However, less evident is the attribution of the continuous decrease of the C−H band frequency (down to ∼2975 cm^{-1}) as temperature decreases to ∼200 K. As explained in Section 1.2, excess ethanol is believed to be excluded from the growing ice phase toward the surface of the grains of the particle through grain boundaries or microstructural defects. This contributes to increase the concentration of an aqueous solution of ethanol dispersed (in a non-crystallized form) around the ice particle, thus shifting the C−H band to lower frequencies. Below 200 K, the C−H band frequencies remain almost constant as the composition of the coexisting aqueous solution (between points 3 and 4, Figure 2) changes less significantly than between 2 and 3. Therefore, crystalline ice is believed to coexist with a supercooled ethanol aqueous solution which has undergone a non-homogeneous increase of concentration between ∼250 and 88 K. Note that using our calibration curve (Figure 1 in Facq et al.[21]), the $\nu_A(CH_3)$ and FR(CH_2) band position at ∼2975 cm^{-1} between ∼200 and 88 K confirms that the concentration of ethanol is high (∼65 wt %) in the remaining liquid layer. Further, we do not exclude the possible formation of an amorphous solid below 97 K (T_g). Our assumption resembles that of Boutron and Kaufmann[13] in that their hexagonal ice was supposed to coexist with an amorphous phase (at temperature below T_g) with a greater concentration of ethanol than in the initial solution in their quenched solution (first cooling) of composition ∼ 25 wt %. As they did not report any other crystalline phase than ice, their supposed co-existing amorphous phase of eutectic concentration did not crystallize. Note that in their X-ray diffraction experiments, Takamuku et al.[17] did not report any other phase than ice with a sample at 22.1 wt % ethanol, but they limited their studies to between 278 and 243 K.

Therefore, the hypothesis derived from the phase diagram discussed in Section 1.2 (Figure 1, blue path), where ice co-exists with an ethanol hydrate and pure ethanol solid (in the studied range between 0 wt % and ∼34 wt % ethanol), seems kinetically inhibited, as no hydrates are reported.

3.3.2. X-ray Diffraction Measurements. Hexagonal ice is seen to occur before 237 K and is stable down to 100 K (Figures 8 and 10). The crystallization temperature of hexagonal ice is here lower than the one observed in the Raman experiment (i.e., ∼248 K with 8.7 wt % ethanol) due to differences in the starting material composition: ∼21 wt % ethanol is used in the X-ray experiment. This is in agreement with literature data[17] that reported hexagonal ice at 243 K in an ethanol solution of 22.1 wt %. Further, it is to notice that except

dx.doi.org/10.1021/jp4015614 | J. Phys. Chem. A 2013, 117, 4916−4927

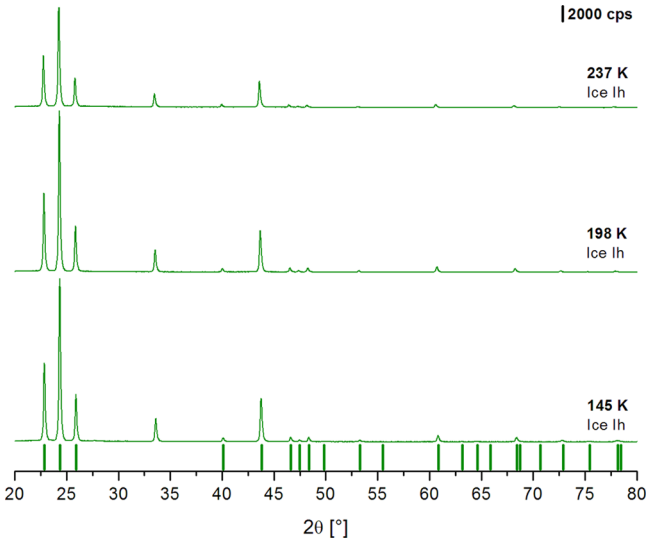

Figure 8. Diffraction pattern of a ∼21 wt % sample recorded during cooling at 1 K·min^{-1} at 237, 198, and 145 K (ice Ih). Green tickmarks represent expected reflections for the known structure of hexagonal ice (derived from Yousuf et al.[32] at 90 K).

for hexagonal ice, no other crystalline phases are detected within this sample, even at the slow cooling rate applied of 1 K·min^{-1}. Additionally, X-ray diffraction experiments were carried out on a quench-cooled ∼8.6 wt % ethanol. As foreseen at this low ethanol concentration, only hexagonal ice is observed at 100 K. The expected ethanol hydrate phases are apparently kinetically inhibited at slow (or high) cooling rate due to the low molecular mobility below 200 K.

3.4. Annealing of the 8.7 wt % Ethanol Aqueous Solution. *3.4.1. O–H and C–H Stretching Modes.* As the main contribution to the Raman spectra is hexagonal ice, the ν_S(OH) band position reflects principally that of pure ice and shows a progressive increase of $\partial\omega/\partial T \sim 0.2$ cm^{-1}·K^{-1} (Figure 9). The melting of ice between 268 and 273 K (points E and F, Figure 9) can be observed as a steep frequency shift of more than 66 cm^{-1}.

On the other hand, the ethanol C–H stretching modes provide additional information on the behavior of the sample during annealing (Figure 9, bottom). Indeed, the $\nu_A(CH_3)$ and FR(CH_2) band exhibits multiple changes of frequency during annealing and notably one frequency redshift between 113 and 123 K. This one is attributed to the crystallization of the remaining liquid solution into a solid hydrate (actually, a new hydrate (IV), see below). A subsequent and progressive blue shift between 158 K and ∼183 K is attributed to the formation of a distinct hydrate (actually hydrate II, see below). The small redshift between 150 and 160 K may result from the dissociation of the first hydrate formed. From 208 to 268 K, a progressive blue–shift follows and is attributed to the evaporation of aqueous ethanol which coexists with hexagonal ice up to 268 K.

3.4.2. X-ray Diffraction Measurements. The behavior observed in Raman experiments is being corroborated by the X-ray diffraction annealing experiments on the previously cooled samples of composition 21 wt % and 8.6 wt % ethanol. In Figure 10, diffractograms from annealed 21 wt % EtOH sample are displayed at 100 K, 150 and 185 K. They show the presence of ice Ih at 100 K and the occurrence of distinct phases as temperature increases. A new phase starts to grow at ∼142 K and is seen to coexist with ice Ih at 150 K. The new phase shows distinct lines in comparison to that of the modified clathrate type I, hydrate II, or even hydrate III identified by Facq et al.[21] New 2θ lines are observed, e.g., at 23.5, 26.6, 27.1, and 45.1°. Further, this new phase vanishes at ∼158 K (not shown here), which corresponds to a temperature very close to the melting point of pure ethanol (monoclinic phase)[33] and seems in agreement with the phase diagram and the trajectories discussed in Section 1.2. To assign properly the new phase observed, we collect a diffraction pattern of crystalline pure ethanol at 145 K (monoclinic phase). Unfortunately, this latter

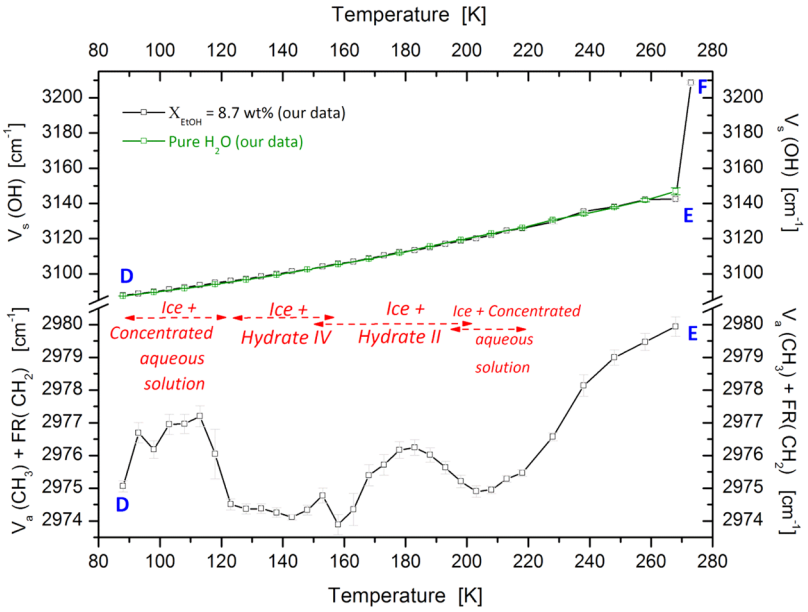

Figure 9. Top: Frequency evolution during annealing from 88 to 268 K of the ν_S(OH) band for pure crystalline ice formed from liquid (open green squares) and a 8.7 wt % EtOH aqueous solution (open black squares). Bottom: Frequency evolution during annealing from 88 to 268 K of the $\nu_A(CH_3)$ and FR(CH_2) band for a 8.7 wt % EtOH aqueous solution (open black squares).

dx.doi.org/10.1021/jp4015614 | J. Phys. Chem. A 2013, 117, 4916–4927

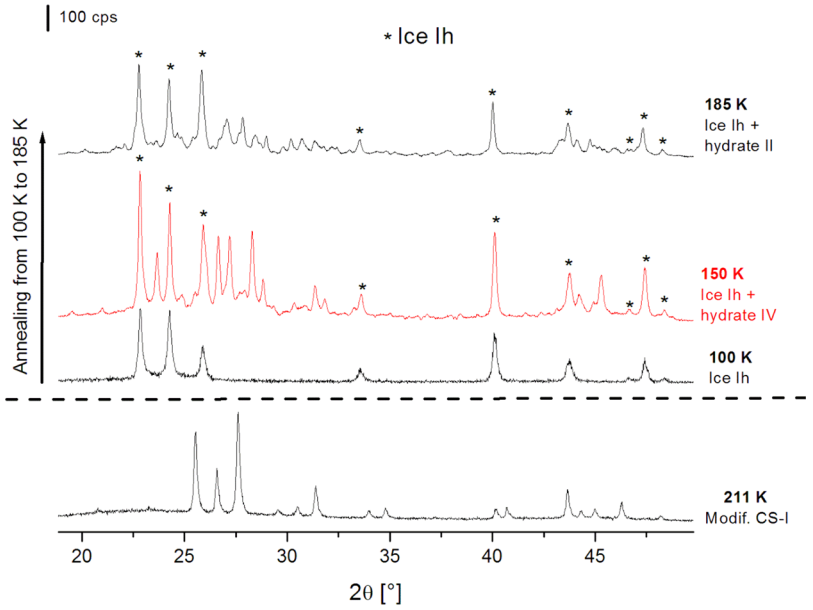

Figure 10. Diffraction patterns of a 21 wt % ethanol sample recorded at 100 K, 150 K (and quenched at 110 K), and 185 K during annealing. Bottom: Diffraction pattern of a 46.5 wt % ethanol sample recorded at 211 K plotted for comparison (taken from Figure 4).

does not match the pattern of the new phase observed in the 21 wt % sample. This means that a new ethanol hydrate of low hydration number (i.e., high ethanol content) has crystallized, and we numbered this phase "ethanol hydrate IV". Upon subsequent cooling down to 100 K and further heating at 155 K, this phase remains stable. The calculation of the peak indexing procedure suggests that the crystal is probably of orthorhombic structure with space group *Pmmm*. The lattice parameters derived from the refinement (figure of merit M'20 = 516 and M20 = 129) are a = 16.37 Å, b = 3.86 Å, and c = 3.34 Å. Upon further annealing above ∼160 K (a temperature that also depends on initial concentration (e.g., ∼155 K for the 8.7 wt %) as reported in the Raman C−H evolution, Figure 9), it decomposes and the ethanol hydrate II starts to grow. The hydrate II reaches its final stage of transformation at 185 K. Then, it decomposes at ∼200 K and only ice Ih remains and coexists with an ethanol aqueous solution until 220 K, where ice begins to dissociate. This also falls in agreement with the behavior observed in the Raman experiment (Figure 9), however, using a sample of somewhat lower concentration. In comparison, Boutron and Kaufmann did not report any new hydrates between 145 and 160 K by X-rays for their 25 wt % sample. But during annealing at ∼180 K, they observed the formation of a "modified clathrate II" (cubic unit cell of 16.3 Å and composition of E·17H_2O). However, their DSC work reveals the presence of two exothermic peaks (crystallization), Td_{01} at 149 K and Td_0 at 171 K, in their thermograms. If Td_0 was attributed to the formation of their supposed "modified clathrate II", they could not establish the origin of the second peak at that time. Td_{01} could well correspond to the formation of the ethanol hydrate IV we observed here at ∼150 K. Because our hydrate II presents ∼25 additional Bragg lines in comparison to that of the "modified CS−II" in our improved X-ray experiments, we believe that the existence of the "modified CS−II" is suspicious. Therefore, Td_0 could well correspond to the formation of the hydrate II.

In summary, the first solid formed during cooling is hexagonal ice as suggested by Takaizumi and Wakabayashi[14] and confirmed by our Raman and X-ray diffraction measurements. According to the frequency shifts observed in the ethanol C−H stretching modes, ice seems to coexist around 200 K and below with an aqueous solution of ethanol concentration higher than the initial solution. This solution remains liquid (or amorphous below 97 K) even at the lowest temperature investigated. The crystallizations of ethanol hydrates IV and II occur upon annealing and are observed both spectroscopically and by X-rays. Note that, only in rare cases, a small proportion of the ethanol hydrate IV has been obtained on quenched cooled samples at 100 K in coexistence with ice Ih. The dissociation of these two hydrates is spectroscopically well established through the spectral modifications recorded in the ethanol C−H stretching modes at ∼160 K and ∼200 K, respectively. This is further confirmed by the distinct diffraction patterns recorded in the corresponding temperature range.

We suggest that the structures given by Boutron and Kaufmann for the solid they formed using a ∼25 wt % mixture by quenching−annealing may have been erroneously attributed to a modified clathrate type II and that the hydrate IV has been overlooked.

4. SUMMARY AND CONCLUSION

The structural evolution of droplets of EtOH aqueous solutions of 8.7 and 46.5 wt % concentration has been investigated on a wide temperature range (253−88 K) using both in situ micro-Raman spectroscopy and X-ray diffraction. The structures formed during cooling and annealing have been identified using the spectral changes observed in the water O−H and ethanol C−H stretching modes and the corresponding changes observed in the diffraction patterns. The micro-Raman analysis provides precise information on the temperature evolution of the structure and on compositional changes in the samples.

At high initial ethanol content (∼46 wt %), a modified type I clathrate (S.G. *Pm*3*m*) is formed at 211 K during cooling. This hydrate remains present down to 88 K and subsequent annealing up to 143 K. A structural rearrangement is then observed between 143 and 173 K. The ethanol hydrate II

dx.doi.org/10.1021/jp4015614 | J. Phys. Chem. A 2013, 117, 4916−4927

(recently identified[20,21]) is formed at 173 K in accordance with the phase diagram. This latter further dissociates at ∼200 K where only ice Ih remains with an aqueous solution of high ethanol content. Ice is then seen to dissociate above 220 K, and the concentration of the ethanol aqueous solution reduces from ∼44 wt % at 228 K to ∼39 wt % at 258 K (as derived from the C−H band frequencies).[21]

Ice Ih is the first solid that forms during cooling of the 8.7 wt % and 21 wt % samples. Ice is shown to coexist with an aqueous solution (or amorphous mixture at low T) of high ethanol content during further cooling down to ∼88 K. Upon annealing, a new hydrate (hydrate IV, S.G. *Pmmm*, orthorhombic) is formed between ∼123 K and ∼142 K and transforms between ∼150 K and ∼158 K into the ethanol hydrate II. At ∼200 K, the hydrate II starts to dissociate, and ice Ih remains with an aqueous layer of high ethanol content. Ice begins to dissociate above ∼220 K.

It is therefore suggested that the freezing of droplets of ethanol aqueous solutions of concentrations lower than 34.4 wt %[14] leads to the formation of a complex crystalline ice particle covered with a supercooled layer of relatively high ethanol content or with an ethanol hydrate and a supercooled layer of high ethanol content. Each case depends on temperature trajectories. The surface reactivity of such a particle (different from the pure ice case) may be taken into account in a number of atmospheric processes. For example, the water uptake of these aerosols, as well as the ice nucleation and ice crystal growth or even the heterogeneous reactions at the surface, can be significantly modified at upper tropospheric temperatures. The behavior highlighted here demonstrates a significant difference in comparison to that occurring in aqueous solutions of organics of high molecular weight (e.g., glucose, raffinose, levoglucosan, carboxylic acids, etc.) that are known to form glasses upon freezing.[23]

One infers that the behavior we reported here can be applied to a number of other species for which the glass transition line (T_g) as a function of concentration does not cross the (metastable) liquidus line in their respective phase diagrams. For, e.g., methanol with T_g = 103 K,[34] *n*-butanol with T_g = 118 K,[35] or *n*-propanol with T_g = 98 K[36,37] exhibit glass transition at relatively low temperature so that the formation of glasses is very unlikely in tropospheric conditions. For these compounds too, the presence of a supercooled (or hydrate) layer can be expected and may influence a number of processes of atmospheric interest. Recently, it has been suggested that the scavenging of trace gases is significantly enhanced on ice surface doped with nitric acid, in contrast to a pure ice surface.[9,10] This effect appears to be promoted by the exclusion of nitric acid to the air−ice interface forming an aqueous liquid layer that favors the dissolution of trace gas species up to the saturated solubility, i.e., much more than that expected in bulk ice.

Finally, one should take into account that our results concern mostly bulk phenomena, and the behavior observed at low temperature may be different in the case of smaller particles of few micrometers radii.[38] More specifically, kinetic barriers due to, e.g., surface tension have a strong effect on the nucleation and crystal growth of phases during the freezing of such particles. This leads to significant differences in the aerosol phase diagram compared to that of the bulk material (e.g., in the liquid−solid phase boundaries).[39]

AUTHOR INFORMATION

Corresponding Author

*B.C.: E-mail: bertrand.chazallon@univ-lille1.fr. Phone: +33 (0)320336468. Fax: +33 (0)320336463.

Present Address

§S.F.: Laboratoire de Géologie de Lyon: Terre, planètes, environnement (UMR 5276), ENS de Lyon, UCB Lyon1, CNRS, 2 rue Raphael Dubois, 69622 Villeurbanne, France.

Notes

The authors declare no competing financial interest.

ACKNOWLEDGMENTS

The authors would like to thank the French national program PNCA-LEFE-CHAT for financial support.

REFERENCES

(1) Fahy, G. M.; Wowk, B.; Wu, J.; Phan, J.; Rasch, C.; Chang, A.; Zendejas, E. Cryopreservation of Organs by Vitrification: Perspectives and Recent Advances. *Cryobiology* **2004**, *48*, 157−178.

(2) Margesin, R.; Neuner, G.; Storey, K. B. Cold-Loving Microbes, Plants, and Animals−Fundamental and Applied Aspects. *Naturwissenschaften* **2007**, *94*, 77−99.

(3) Koop, T. Homogeneous Ice Nucleation in Water and Aqueous Solutions. *Z. Phys. Chem.* **2004**, *218*, 1231−1258.

(4) Kley, D. Tropospheric Chemistry and Transport. *Science* **1997**, *276*, 1043−1045.

(5) Singh, H. B.; Kanakidou, M.; Crutzen, P. J.; Jacob, D. J. High-Concentrations and Photochemical Fate of Oxygenated Hydrocarbons in the Global Troposphere. *Nature* **1995**, *378*, 50−54.

(6) Singh, H. B.; Chen, Y.; Staudt, A.; Jacob, D. J.; Blake, D.; Heikes, B.; Snow, J. Evidence From the Pacific Troposphere for Large Global Sources of Oxygenated Organic Compounds. *Nature* **2001**, *410*, 1078−1081.

(7) Singh, H. B.; Salas, L. J.; Chatfield, R. B.; Czech, E.; Fried, A.; Walega, J.; Evans, M. J.; Field, B. D.; Jacob, D. J.; Blake, D.; et al. Analysis of the Atmospheric Distribution, Sources, and Sinks of Oxygenated Volatile Organic Chemicals Based on Measurements Over the Pacific During TRACE-P. *J. Geophys. Res.* **2004**, *109* (D15), 19201.

(8) Wisthaler, A.; Hansel, A.; Dickerson, R. R.; Crutzen, P. J. Organic Trace Gas Measurements by PTR-MS During INDOEX 1999. *J. Geophys. Res.* **2002**, *107* (D19), 8024.

(9) Kerbrat, M.; Le Calvé, S.; Mirabel, Ph. Uptake Measurements of Ethanol on Ice Surfaces and on Supercooled Aqueous Solutions Doped with Nitric Acid Between 213 and 243 K. *J. Phys. Chem. A* **2007**, *111*, 925−931.

(10) Petitjean, M.; Mirabel, P.; Le Calvé, S. Uptake Measurements of Acetaldehyde on Solid Ice Surfaces and on Solid/Liquid Supercooled Mixtures Doped with HNO_3 in the Temperature Range 203−253 K. *J. Phys. Chem. A* **2009**, *113*, 5091−5098.

(11) Vuillard, G.; Satragno, N. Sur un Hydrate de l'Ethanol. *Comptes Rendus* **1960**, *250*, 3841−3843.

(12) Potts, A. D.; Davidson, D. W. Ethanol Hydrate. *J. Phys. Chem.* **1965**, *69*, 996−1000.

(13) Boutron, P.; Kaufmann, A. Metastable States in the System Water−Ethanol. Existence of a Second Hydrate; Curious Properties of Both Hydrates. *J. Chem. Phys.* **1978**, *68*, 5032−5041.

(14) Takaizumi, K.; Wakabayashi, T. The Freezing Process in Methanol−, Ethanol−, and Propanol−Water Systems as Revealed by Differential Scanning Calorimetry. *J. Solution Chem.* **1997**, *26*, 927−939.

(15) Murthy, S. S. N. Detailed Study of Ice Clathrate Relaxation: Evidence for the Existence of Clathrate Structures in Some Water−Alcohol Mixtures. *J. Phys. Chem. A* **1999**, *103*, 7927−7937.

(16) Zelenin, Y. M. Effect of Pressure on Clathrate Formation in a Water−Ethanol System. *J. Struct. Chem.* **2003**, *44*, 130−136.

(17) Takamuku, T.; Saisho, K.; Nozawa, S.; Yamaguchi, T. X-ray Diffraction Studies on Methanol−Water, Ethanol−Water, and 2−Propanol−Water Mixtures at Low Temperatures. *J. Mol. Liq.* **2005**, *119*, 133−146.
(18) Takaizumi, K. A Curious Phenomenon in the Freezing−Thawing Process of Aqueous Ethanol Solution. *J. Solution Chem.* **2005**, *34*, 597−612.
(19) Chazallon, B.; Celik, Y.; Focsa, C.; Guinet, Y. Vapor Deposited Ethanol−H_2O Ice Mixtures Investigated by Micro−Raman Scattering. *Vib. Spectrosc.* **2006**, *42*, 206−214.
(20) Chazallon, B.; Focsa, C.; Capet, F.; Guinet, Y. Ethanol Hydrates Formed by Gas-Condensation: Investigations by Raman Scattering and X-ray Diffraction. *Physics and Chemistry of Ice*; Kuhs, W. F., Ed.; Royal Society of Chemistry: Cambridge, U.K., 2007; pp 133−140.
(21) Facq, S.; Danède, F.; Chazallon, B. Ethanol Hydrates and Solid Solution Formed by Gas Condensation: An in Situ Study by Micro−Raman Scattering and X-ray Diffraction. *J. Phys. Chem. A* **2010**, *114*, 10646−10654.
(22) Corti, H.; Austen Angell, C.; Auffret, T.; Levine, H.; Pilar Buera, M.; Reid, D. S.; Roos, Y. H.; Slade, L. Empirical and Theoretical Models of Equilibrium and Non−Equilibrium Transition Temperatures of Supplemented Phase Diagrams in Aqueous Systems (IUPAC Technical Report). *Pure Appl. Chem.* **2010**, *82*, 1065−1097.
(23) Zobrist, B.; Marcolli, C.; Pedernera, D. A.; Koop, T. Do Atmospheric Aerosols Form Glasses? *Atmos. Chem. Phys.* **2008**, *8*, 5221−5244.
(24) Jensen, E. J.; Smith, J. B.; Pfister, L.; Pittman, J. V.; Weinstock, E. M.; Sayres, D. S.; Herman, R. L.; Troy, R. F.; Rosenlof, K.; Thompson, T. L.; et al. Ice Supersaturations Exceeding 100% at the Cold Tropical Tropopause: Implications for Cirrus Formation and Dehydration. *Atmos. Chem. Phys.* **2005**, *5*, 851−862.
(25) Altomare, A.; Caliandro, R.; Camalli, M.; Cuocci, C.; Giacovazzo, C.; Moliterni, A. G. G.; Rizzi, R. Automatic Structure Determination From Powder Data with EXPO2004. *J. Appl. Crystallogr.* **2004**, *37*, 1025−1028.
(26) Johari, G. P.; Chew, H. A. M. Pressure and Temperature−Dependence of the O−H and O−D Stretching Vibrations in the Raman−Spectrum of Ice. *Philos. Mag. B* **1984**, *49*, 647−660.
(27) Whalley, E. Detailed Assignment of O−H Stretching Bands of Ice I. *Can. J. Chem.* **1977**, *55*, 3429−3441.
(28) Sivakumar, T. C.; Rice, S. A.; Sceats, M. G. Raman−Spectroscopic Studies of OH Stretching Region of Low−Density Amorphous Solid Water and of Polycrystalline Ice Ih. *J. Chem. Phys.* **1978**, *69*, 3468−3476.
(29) Wong, P. T. T.; Whalley, E. Optical-Spectra of Orientationally Disordered Crystal. 5. Raman−Spectrum of Ice Ih in the Range 4000−350 cm^{-1}. *J. Chem. Phys.* **1975**, *62*, 2418−2425.
(30) Mizuno, K.; Miyashita, Y.; Shindo, Y. NMR and FT−IR Studies of Hydrogen−Bonds in Ethanol−Water Mixtures. *J. Phys. Chem.* **1995**, *99*, 3225−3228.
(31) Yu, Y.; Lin, K.; Zhou, X.; Wang, H.; Liu, S.; Ma, X. New C−H Stretching Vibrational Spectral Features in the Raman Spectra of Gaseous and Liquid Ethanol. *J. Phys. Chem. C* **2007**, *11*, 8971−8978.
(32) Yousuf, M.; Qadri, S. B.; Knies, D. L.; Grabowski, K. S.; Coffin, R. B.; Pohlman, J. W. Novel Results on Structural Investigations of Natural Minerals of Clathrate Hydrates. *Appl. Phys. A: Mater. Sci. Process.* **2004**, *78*, 925−939.
(33) Jönsson, P. G. Hydrogen Bond Studies. CXIII. The Crystal Structure of Ethanol at 87 K. *Acta Crystallogr., Sect. B: Struct. Crystallogr. Cryst. Chem.* **1976**, *32*, 232−235.
(34) Sugisaki, M.; Suga, H.; Seki, S. Calorimetric Study of Glassy State. 3. Novel Type Calorimeter for Study of Glassy State and Heat Capacity of Glassy Methanol. *Bull. Chem. Soc. Jpn.* **1968**, *41*, 2585−2591.
(35) Faucher, J. A.; Koleske, J. V. Glass Transitions of Organic Compounds. 1 . Lower Aliphatic Alcohols. *Phys. Chem. Glasses* **1966**, *7*, 202−208.
(36) Angell, C. A.; Smith, D. L. Test of the Entropy Basis of the Vogel−Tammann−Fulcher Equation − Dielectric−Relaxation of Polyalcohols Near Tg. *J. Phys. Chem.* **1982**, *86*, 3845−3852.
(37) Yatsu, A.; Kojima, S.; Suzuki, T. Study of Glass−Transition of Propanol by Photoacoustic Method. *Jpn. J. Appl. Phys.* **1994**, *33*, 3230−3233.
(38) Facq, S.; Ph. D. Thesis, Université Lille1, 2011.
(39) Dickens, D. B.; Sloan, J. J. The Nucleation and Freezing of Dilute Nitric Acid Aerosols. *J. Phys. Chem. A* **2002**, *106*, 10543−10549.